

Secure Over-the-Air Computation Against Multiple Eavesdroppers using Correlated Artificial Noise

David Nordlund, *Student Member, IEEE*, Luis Maßny, *Student Member, IEEE*, Antonia Wachter-Zeh, *Senior Member, IEEE*, Erik G. Larsson, *Fellow, IEEE*, and Zheng Chen, *Senior Member, IEEE*

Abstract—In the era of the Internet of Things and massive connectivity, many engineering applications, such as sensor fusion and federated edge learning, rely on efficient data aggregation from geographically distributed users over wireless networks. Over-the-air computation shows promising potential for enhancing resource efficiency and scalability in such scenarios by leveraging the superposition property of wireless channels. However, due to the use of uncoded transmission with linear mapping, it also suffers from security vulnerabilities that must be dealt with to allow widespread adoption. In this work, we consider a scenario where multiple cooperating eavesdroppers attempt to infer information about the aggregation result. We derive the optimal joint estimator for the eavesdroppers and provide bounds on the achievable estimation accuracy for both the eavesdroppers and the intended receiver. We show that significant inherent security exists against individual eavesdroppers due to channel misalignment. However, the security level is greatly compromised when the eavesdroppers can cooperate, motivating the need for deliberate security measures. A common measure is to add carefully calibrated perturbation signals (artificial noise) prior to data transmission to improve the security level. To this end, we propose a zero-forced artificial noise design that achieves a high level of security against cooperative eavesdroppers without compromising the aggregation accuracy.

Index Terms—Over-the-air computation, secure communication, correlated artificial noise, optimization.

I. INTRODUCTION

Recent advances in artificial intelligence (AI) services and applications are shaping the next generation of communication network designs. Many distributed AI applications, such as federated learning (FL) [1], rely on iterative information exchange between (potentially large numbers of) distributed nodes and a central server. Naturally, a communication bottleneck arises when the information exchange process is constrained by limited resources, such as frequency-time resource blocks in wireless systems. Over-the-Air (OtA) computation has been proposed to address this issue [2]–[8] and has recently received particular attention for FL applications [9]–[13]. OtA computation leverages the superposition property of multiple access channels, which enables the computation of various nomographic functions (e.g., the sum) of distributed data without allocating orthogonal resources to each source node [14]. Consequently, the system is innately scalable in the number of transmitting nodes.

Research in OtA computation has grown considerably in recent years. In the current literature, there are many variants of OtA schemes, depending on the nature of information sources (analog or digital), data processing designs (coded or uncoded), and the availability of channel state information (for coherent or non-coherent combining). In this work, we focus on analog OtA computation with linear precoding and coherent processing. Analog OtA computation with uncoded transmission faces additional security and privacy issues that are not encountered in conventional digital wireless communication systems. In particular, the scheme limits the possibility for digital encryption and advanced coding schemes, rendering it vulnerable to eavesdropping. In modern information networks, data security is achieved primarily through cryptographic primitives applied to digital data at the upper layers of the protocol stack [15]. When the physical signals are to be protected, additional mechanisms need to be introduced to safeguard communication against eavesdropping, which has been researched in the domain of physical layer security [16], [17]. However, unlike digital communication protocols for point-to-point or multiple-access channels, analog OtA computation requires phase and amplitude alignment to ensure coherent signal aggregation at the receiver and imposes per-user power constraints. This results in novel design challenges that require re-engineering of the processing chain.

The problem of physical layer security has been approached from different perspectives in the literature. The domain of *information-theoretic security* for the physical layer studies equivocation and mutual information rates for the wiretap channel [18]. Existing works focus on the fundamental limits of those quantities and rely primarily on non-constructive channel coding techniques, e.g., [19], [20]. A similar but more practical approach is *estimation-theoretic security*, which aims at preventing an eavesdropper from accurately estimating a secret [21], [22], measured by the eavesdropper's Mean Squared Error (MSE). Perfect information-theoretic secrecy (zero mutual information) implies that an eavesdropper's observation is statistically independent from the secret. In contrast, having a maximal MSE implies that an eavesdropper cannot estimate the secret more accurately (in the MSE sense) than from its prior knowledge; however, this does not necessarily induce statistical independence. Estimation- and information-theoretic security can be related through the connection between the MSE and the mutual information. For instance, for additive Gaussian channels, the minimum MSE equals twice the derivative of the mutual information w.r.t. the Signal-to-Noise-Ratio (SNR) [23]. Moreover, the secret's entropy yields a lower bound on the MSE [24, Theorem 8.6.6].

D. Nordlund, E. G. Larsson and Z. Chen are with Linköping University, Dept. of Electrical Engineering (ISY), Division of Communication Systems, 581 83 Linköping, Sweden (emails: david.nordlund@liu.se, erik.g.larsson@liu.se, zheng.chen@liu.se).

L. Maßny and A. Wachter-Zeh are with the School of Computation, Information and Technology at the Technical University of Munich, 80333 Munich, Germany (emails: luis.massny@tum.de, antonia.wachter-zeh@tum.de)

Common approaches on estimation-theoretic security includes the design of transmit and receive filters [25], cooperative jamming [26], cooperative precoding [27], and beamforming [28]. Another popular idea for physical layer security is to leverage artificial noise to interfere with the eavesdropper [29]–[32]. Particularly, artificial noise has been extensively studied in the context of differentially private [33] FL with OtA computation, in both single-antenna [34]–[38] and multiple-antenna [39] systems. In this scenario, noise is injected to protect local gradients from revealing information about the training dataset [40].

In our work, we aim at protecting the intended computation result of an OtA computation against eavesdroppers while ensuring a high level of aggregation accuracy at the legitimate receiver.¹ Following the estimation-theoretical approach in prior works [14], [25], [32], [41], we measure accuracy and security in terms of the MSE at the legitimate receiver and at the eavesdroppers, respectively.

A. Closely Related Works

Secure OtA computation has been studied in several prior works using cooperative jamming and artificial noise. In [42], a friendly jammer, whom the server can perfectly compensate for, is leveraged to degrade the eavesdropper's estimation performance. The receiver itself can act as a friendly jammer when full-duplex receivers are available [43]–[45], as it can perfectly cancel the jamming signal locally. Alternatively, [46] considers selecting a subset of the users to act as jammers. The drawback of this scheme is that some users are excluded from participating in the computation process, which disqualifies it for our purposes. In [47], a joint source-channel coding scheme is proposed for information-theoretic security. However, the analysis is limited to linear discrete channels.

Following the artificial noise approach, both correlated [41], [48], [49] and uncorrelated [34], [35] noise designs have been considered in the literature. Particularly, adding spatially correlated noise across multiple users enables noise cancellation towards the intended receiver, thereby improving aggregation accuracy [48], [49]. Additionally, [41] considers a full-duplex adversary acting as both eavesdropper and jammer and proposes a numerical algorithm to jointly design power allocation, user selection, artificial noise, and receiver filters. The approach of correlated artificial noise can be interpreted as joint beamforming across distributed antennas. A similar concept is considered in [50], which introduces a distributed null-steering beamforming scheme aimed at maximizing the MSE at the eavesdropper, although it relies on knowledge of the eavesdropper's location. In this work, we extend the study of correlated artificial noise schemes to the case when multiple (potentially cooperating) eavesdroppers exist in the system. We require all users to participate in the computation and consider half-duplex transceivers.

¹We distinguish the problem of protecting the computation result from the problem of protecting the input data, even though solutions to the latter problem would be applicable to the former.

B. Technical Contributions

Our specific contributions are as follows.

- Assuming Gaussian distributed source data, we provide *bounds on the expected achievable MSE* at the eavesdroppers and at the server, in both cooperative and non-cooperative (eavesdropping) cases.
- Furthermore, we provide an *optimal joint estimator for cooperative eavesdroppers* when they have exact channel state information. In an alternative case where they only have statistical information about the channels, and the phase follows a uniform distribution, we show that the system is secure even without adding extra artificial noise.
- We illustrate the inherent security against eavesdropping in OtA systems, due to channel phase misalignment. Subsequently, we show that this security is compromised in the presence of cooperating eavesdroppers, motivating the need for deliberate security measures.
- Lastly, we propose an *optimized artificial noise design* for the non-cooperative case, which also demonstrates strong security performance in the cooperative case, as shown in numerical simulations.

C. Paper Organization

The rest of the paper is organized as follows. Section II introduces the security and accuracy metrics, provides an overview of the system, and discusses the power control design and performance measures of the legitimate receiver. Section III provides the security bound and optimal strategy of the eavesdroppers. In Section IV, we detail our proposed artificial noise design. Simulation results are presented in Section V, and the work is summarized in Section VI.

D. Notation

Vectors and matrices are denoted by bold lower case and upper case symbols, respectively. All vectors are column vectors. $(\cdot)^H$ denotes complex conjugate transpose, $(\cdot)^*$ complex conjugate, $\|\cdot\|$ the ℓ^2 norm and $\mathcal{CN}(\cdot, \cdot)$ the complex Gaussian distribution.

II. SYSTEM MODEL

As shown in Fig. 1, we consider a wireless system in which local data from K distributed users must be aggregated at a central server using over-the-air (OtA) computation over a multiple-access block fading channel. Let $\gamma = (\gamma_1, \dots, \gamma_K) \in \mathbb{C}^K$ represent the source data vector, where $\gamma_k \in \mathbb{C}$ is the source data of user $k \in \{1, \dots, K\}$.² We assume $\gamma \sim \mathcal{CN}(\mathbf{0}, \mathbf{I}_K)$, meaning that the source data from all users follow independent Gaussian distributions and are normalized prior to transmission. The goal is to compute the function $s = f(\gamma_1, \dots, \gamma_K) = \sum_{k=1}^K \gamma_k$. Note that this framework can easily be extended to any weighted sum instead of the sum.

The joint communication-computation processing chain can be divided into three main parts:

²If the original data is real-valued, it can be split into two streams that are then combined into one complex stream.

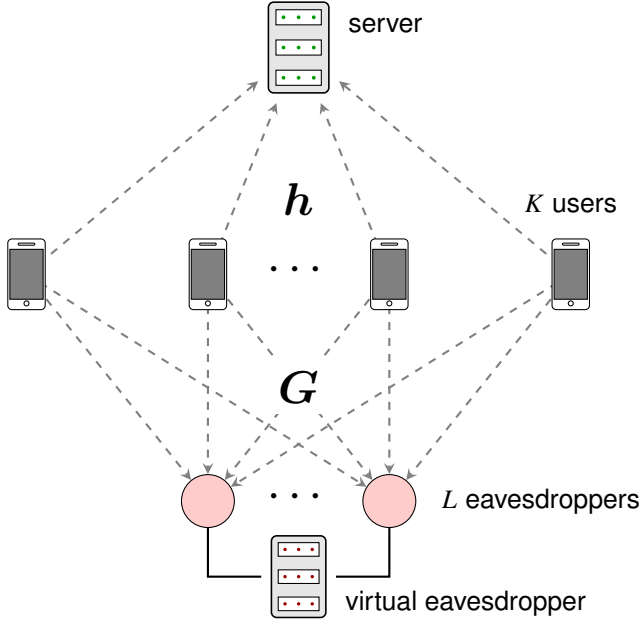


Fig. 1. Overview of the system. Wireless transmissions (dashed arrows), intended for the server, are overheard by L eavesdroppers that jointly process their received signals at a *virtual eavesdropper*. The solid lines represent an error-free channel.

TABLE I
NOTATION

K	number of legitimate users
L	number of eavesdroppers
$\gamma = (\gamma_1, \dots, \gamma_K)^T \in \mathbb{C}^{K \times 1}$	source data
$s = \sum_{k=1}^K \gamma_k \in \mathbb{C}$	the target function
$\mathbf{h} \in \mathbb{C}^{K \times 1}$	server channel vector
$\mathbf{G} \in \mathbb{C}^{L \times K}$	eavesdroppers channel matrix
$y \in \mathbb{C}$	received value at the server
$z_\ell \in \mathbb{C}$	received value at the ℓ -th eavesdropper
$D \in [0, 1]$	approximation error
$S \in [0, 1]$	security level
$\mathbf{A} \in \mathbb{C}^{K \times m}$	artificial noise precoding matrix
$\mathbf{w} \in \mathbb{C}^{K \times 1}$	artificial noise vector
$\eta \in \mathbb{R}$	amplitude scaling factor
$\mathbf{p} \in \mathbb{C}^{L \times 1}$	eavesdropper combining vector

- 1) encoding/pre-processing data at the source nodes;
- 2) amplitude modulation and signal transmission over analog channels;
- 3) decoding/post-processing of received superimposed signal at the receiver/server.

A typical encoding/pre-processing rule in OtA computation is to perform channel inversion. Let $x_k \in \mathbb{C}$ represent the encoded data symbol from user k , which can be written as

$$x_k = \eta h_k^{-1} \gamma_k, \quad (1)$$

where $h_k \in \mathbb{C}$ is the channel fading coefficient between user k and the server, and η is an (amplitude) scaling factor chosen

to satisfy the power constraints $\mathbb{E}\{|x_k|^2\} \leq P$. The server receives

$$y = \mathbf{h}^T \mathbf{x} + n_y, \quad (2)$$

where $\mathbf{x} = (x_1, \dots, x_K)^T$, $n_y \sim \mathcal{CN}(0, \sigma_y^2)$ is additive noise and $\mathbf{h} = (h_1, \dots, h_K)^T \in \mathbb{C}^K$ contains the corresponding channel coefficients. After receiving the superimposed signal, the server performs linear scaling (post-processing) and obtains an estimate of the intended computation result as

$$\hat{f}(y) = \frac{y}{\eta} = \sum_{k=1}^K \gamma_k + \frac{n_y}{\eta}. \quad (3)$$

The common scaling factor η will determine the estimation noise in the computation result.

In addition to the legitimate users, there exist L eavesdroppers in the system. Each eavesdropper $\ell \in \{1, \dots, L\}$ receives

$$z_\ell = \mathbf{g}_\ell^T \mathbf{x} + n_{z_\ell}, \quad (4)$$

where $n_{z_\ell} \sim \mathcal{CN}(0, \sigma_{z_\ell}^2)$ is additive noise, and $\mathbf{g}_\ell \in \mathbb{C}^K$ is the channel coefficient vector between the K legitimate users and the ℓ -th eavesdropper. The purpose of this work is to investigate the level of secrecy and aggregation accuracy of the system, depending on the strategy employed by the eavesdroppers. Although we consider only single-antenna devices, multiple single-antenna eavesdroppers can be viewed as a virtual eavesdropper with multiple distributed antennas. In particular, we investigate a scenario where the eavesdroppers can jointly post-process their received signals (using an error-free side channel) to obtain an estimate of the sum $s = \sum_{k=1}^K \gamma_k$. Table I provides a summary of the notation used throughout this paper.

A. Accuracy and Security Measures

We adopt the following MSE-based accuracy and security measures.

Definition 1. Let $f : \mathbb{C}^K \rightarrow \mathbb{C}$ be the objective function. For a given channel realization, we say that an OtA computation scheme, operating in the presence of multiple cooperating eavesdroppers, is MSE-approximate with approximation error

$$D = \min_{d_y : \mathbb{C} \rightarrow \mathbb{C}} \frac{\mathbb{E}\{|d_y(y; \Phi) - f(\gamma_1, \gamma_2, \dots, \gamma_K)|^2 | \Phi\}}{\text{Var}\{f(\gamma_1, \gamma_2, \dots, \gamma_K)\}},$$

and MSE-secure with security level

$$S = \min_{d_z : \mathbb{C}^L \rightarrow \mathbb{C}} \frac{\mathbb{E}\{|d_z(z_1, \dots, z_L; \Phi) - f(\gamma_1, \gamma_2, \dots, \gamma_K)|^2 | \Phi\}}{\text{Var}\{f(\gamma_1, \gamma_2, \dots, \gamma_K)\}},$$

where $d_y(\cdot; \Phi)$ and $d_z(\cdot; \Phi)$ are the post-processing functions of the legitimate server and eavesdroppers (jointly) respectively, and $\Phi = \{\Phi_1, \dots, \Phi_L\}$ is some side information about the channels between legitimate users and eavesdroppers. The expectations are taken over the joint distribution of γ , the randomness used in the pre-processing, the fading distribution (if not part of the side information), and the channel noise n_y or $(n_{z_1}, \dots, n_{z_L})$, respectively.

According to this definition, the approximation error is the minimum (normalized) MSE that the server can achieve

(given optimal post-processing), and the security level is a lower bound on the (normalized) MSE that the eavesdroppers can achieve after joint processing, reflecting the maximum information leakage. The approximation error and security level lie in the range $D, S \in [0, 1]$, since normalized MSE with maximum value 1 can be achieved with the naive estimates $d_y(y; \Phi) = \mathbb{E}\{s\}$ and $d_z(z_1, \dots, z_L; \Phi) = \mathbb{E}\{s\}$ respectively. However, we note that even this maximal estimation-theoretic security does not imply that no information can be inferred about the source data from the received signal.

B. Secure Encoder Design

To achieve security against eavesdropping, one common strategy in the literature is to add artificial noise (perturbation signals) prior to signal transmission to hide the true information. Therefore, the encoding scheme can be modified by letting each user k transmit

$$x_k = \eta h_k^{-1} \gamma_k + w_k, \quad (5)$$

where $w_k \in \mathbb{C}$ represents the added artificial noise. We first discuss the artificial noise design and then return to the power control design.

Remark 1. For secure OtA aggregation design, two slightly different operations exist in the literature: adding noise after scaling (cf. [48])

$$x_k^{(A)} = \eta^{(A)} h_k^{-1} \gamma_k + w_k^{(A)}, \quad (6)$$

and adding noise before scaling (cf. [49])

$$x_k^{(B)} = \eta^{(B)} h_k^{-1} (\gamma_k + w_k^{(B)}). \quad (7)$$

These representations are equivalent, since one can always find a set of valid parameters (amplitude scaling factor and artificial noise design) in one framework that corresponds to a set of parameters in the other framework such that $x_k^{(A)} = x_k^{(B)}$. In this work, we use the framework in (6) since it gives an intuitive interpretation of the system design, i.e., one can fix the power of the real data signal through η , then use the remaining power $P - (\eta/h_k)^2$ for security preservation.

1) *Correlated Artificial Noise Design:* Adding artificial noise generally increases the approximation error (aggregation noise perceived at the server). Different correlated noise designs have been proposed to limit (or entirely mitigate) this effect, such as using spatially correlated (or zero-forced) noise such that the received aggregated artificial noise sums to zero at the server. To encompass a variety of such schemes, we consider correlated noise designs of the form

$$\mathbf{w} = (w_1, w_2, \dots, w_K)^T = \mathbf{A}\mathbf{v}, \quad (8)$$

where $\mathbf{A} \in \mathbb{C}^{K \times m}$ is the noise precoding matrix and $\mathbf{v} \in \mathbb{C}^m$ a random vector, for some $m \leq K$.

Remark 2. One particular choice of correlated noise design is the zero-forced noise ($\mathbf{h}^T \mathbf{w} = 0$), which can be achieved by choosing \mathbf{A} such that $\mathbf{h}^T \mathbf{A} = \mathbf{0}$, that is, by letting the columns of \mathbf{A} be orthogonal to \mathbf{h}^* . This can only be achieved when $m < K$.

To facilitate the analysis, we consider Gaussian distributed artificial noise, i.e., $\mathbf{v} \sim \mathcal{CN}(\mathbf{0}, \mathbf{I}_m)$. Using this representation, we can describe the artificial noise by its covariance matrix $\mathbf{Q} = \text{Cov}[\mathbf{w}] = \mathbf{A}\mathbf{A}^H$, where m limits the rank of \mathbf{Q} , or equivalently the subspace in which \mathbf{w} lies.

In practice, users can jointly generate their artificial noise through the following process: the noise matrix \mathbf{A} is generated at the central server and shared with all users, along with a common random seed that is used to locally generate the same pseudo-random noise vector \mathbf{v} . With this, each user k computes their artificial noise as $w_k = [\mathbf{A}\mathbf{v}]_k$. This process motivates the design choice to make \mathbf{A} non-square, since smaller m reduces the overhead cost of sharing \mathbf{A} with all users, at the cost of shrinking its design space.³

2) *The Effects of Power Control:* As stated in Remark 1, the amplitude scaling factor η controls the division of power between the real data signal and artificial noise, i.e., it controls the trade-off between MSE-security and MSE-approximation. Let $\mathbf{a}_1^T, \dots, \mathbf{a}_K^T$ denote the rows of \mathbf{A} , then we have $\mathbb{E}\{|w_k|^2\} = \|\mathbf{a}_k\|^2$. Consequently, the individual power constraints $\mathbb{E}\{|x_k|^2\} \leq P$ yield the following upper bound on the amplitude scaling factor:

$$\eta^2 \leq \min_{k \in \{1, 2, \dots, K\}} |h_k|^2 (P - \|\mathbf{a}_k\|^2). \quad (9)$$

With legitimate users employing the secure encoding design, the server and eavesdroppers receive

$$y = \sum_{k=1}^K (\eta \gamma_k + h_k w_k) + n_y = \eta s + \mathbf{h}^T \mathbf{A} \mathbf{v} + n_y, \quad (10)$$

$$\begin{aligned} z_\ell &= \eta \sum_{k=1}^K \frac{g_{\ell,k}}{h_k} \gamma_k + \mathbf{g}_\ell^T \mathbf{A} \mathbf{v} + n_{z_\ell} \\ &= \eta s + \eta \sum_{k=1}^K \left(\frac{g_{\ell,k}}{h_k} - 1 \right) \gamma_k + \mathbf{g}_\ell^T \mathbf{A} \mathbf{v} + n_{z_\ell}, \quad \forall \ell \in \{1, \dots, L\}, \end{aligned} \quad (11)$$

where s is the intended computation result. Theorem 1 gives the resulting approximation error at the server.

Theorem 1. Consider the proposed OtA computation scheme with source data $\gamma \sim \mathcal{CN}(\mathbf{0}, \mathbf{I}_K)$. The computation result is MSE-approximate with approximation error

$$D = 1 - \frac{\eta^2 K}{\eta^2 K + \|\mathbf{h}^T \mathbf{A}\|^2 + \sigma_y^2}.$$

Proof. See Appendix A. □

Based on this result, Corollary 1 gives the achievable design space for the amplitude scaling factor η , given an upper bound on the approximation error.

³It might seem preferable to directly share the noise vector \mathbf{w} with all users since its dimension is smaller than the noise precoding matrix \mathbf{A} . However, in case the source data contain high-dimensional vectors, it would be much more efficient to share \mathbf{A} instead of \mathbf{w} . Additionally, as will be shown later, \mathbf{A} can be broadcast openly and thus known by the eavesdroppers while still providing some security guarantees.

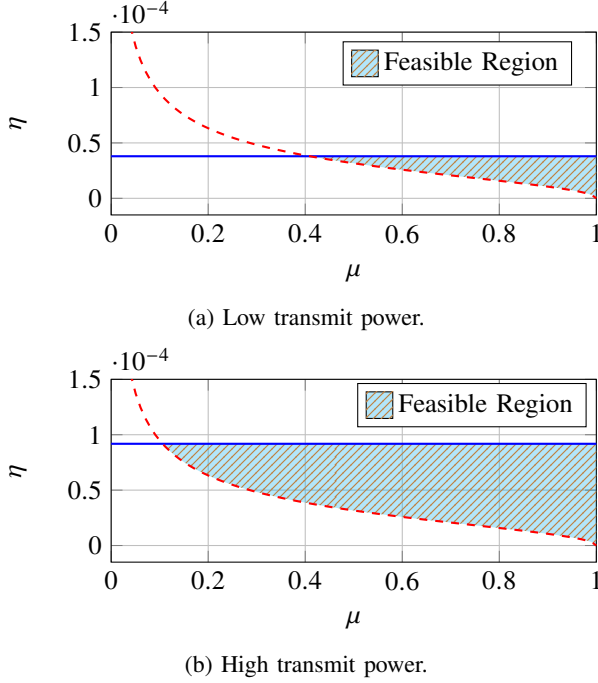


Fig. 2. The shaded area represents the design space for the amplitude scaling factor η under different approximation error constraints. The bounding curves are derived from the upper and lower bounds in Corollary 1.

Corollary 1. For a given upper bound on the approximation error, $D \leq \mu$, the amplitude scaling factor must satisfy

$$\frac{(1 - \mu)(\|\mathbf{h}^T \mathbf{A}\|^2 + \sigma_y^2)}{\mu K} \leq \eta^2 \leq \min_{k \in \{1, 2, \dots, K\}} |h_k|^2 (P - \|\mathbf{a}_k\|^2).$$

Based on Corollary 1, the design space of η is illustrated in Fig. 2. Each point is achievable for some choice of \mathbf{A} . With zero-forced noise, the lower bound is independent of \mathbf{A} , thus yielding the largest feasible region. With other designs, the lower bound increases according to the amount of artificial noise that enters the received signal at the server. This result sheds some light on the intricate relationship between the approximation error and security level. Smaller η increases the power allocated to the artificial noise, thus increasing the security level, but it simultaneously increases the approximation error since less power is allocated to the data. To compensate for that, one can design the artificial noise carefully to reduce $\|\mathbf{h}^T \mathbf{A}\|^2$ (e.g., by zero-forcing), limiting the design space of \mathbf{A} , which might in turn decrease the security level. We will continue this discussion in Section V.

C. Joint Decoder Design at Multiple Eavesdroppers

Based on the received signal at each eavesdropper given in (11), the L eavesdroppers can jointly process their received signals and obtain an estimate of the target function value, denoted by \hat{s} . The security level in Definition 1 is then the normalized expected MSE after joint processing (receive combining). For a given channel realization, the Minimum Mean Squared Error (MMSE) estimator

$$d_{z, \text{opt}} = \arg \min_{d_z: \mathbb{C}^L \rightarrow \mathbb{C}} \mathbb{E} \{ |d_z(z_1, \dots, z_L; \Phi) - s|^2 \},$$

is linear since the observations $\{z_\ell\}_{\ell=1, \dots, L}$ and the estimation target s are jointly Gaussian [51, Prop. 3.9]. Therefore, the target function estimate is $\hat{s} = d_z(z_1, \dots, z_L; \Phi) = \mathbf{p}^H \mathbf{z}$, where $\mathbf{z} = (z_1, \dots, z_L)^T$ and $\mathbf{p} = (p_1, \dots, p_L)^T \in \mathbb{C}^L$ is the combining vector. Being a linear combination of each eavesdropper's received signal, the estimate can be viewed as the decoded signal at a single *virtual eavesdropper*, which is connected to L spatially distributed eavesdroppers.

Introducing notations $\mathbf{n}_z = (n_{z_1}, \dots, n_{z_L})^T$ and

$$\mathbf{D}_h = \begin{bmatrix} h_1 & & 0 \\ & \ddots & \\ 0 & & h_K \end{bmatrix}, \quad \mathbf{G} = \begin{bmatrix} -\mathbf{g}_1^T & - \\ -\mathbf{g}_2^T & - \\ \vdots & \\ -\mathbf{g}_L^T & - \end{bmatrix},$$

we can write the received signal vector \mathbf{z} at the virtual eavesdropper as

$$\mathbf{z} = \eta \mathbf{G} \mathbf{D}_h^{-1} \boldsymbol{\gamma} + \mathbf{G} \mathbf{A} \mathbf{v} + \mathbf{n}_z. \quad (12)$$

The MMSE estimator is

$$\hat{s}_{\text{opt}} = d_{z, \text{opt}}(\mathbf{z}) = \mathbf{p}_{\text{opt}}^H \mathbf{z}, \quad (13)$$

where

$$\mathbf{p}_{\text{opt}} = \arg \min_{\mathbf{p} \in \mathbb{C}^L} \mathbb{E} \{ |\mathbf{p}^H \mathbf{z} - s|^2 \}. \quad (14)$$

With this, the security level in Definition 1 can be equivalently written as

$$S = \frac{\mathbb{E} \{ |\mathbf{p}_{\text{opt}}^H \mathbf{z} - s|^2 \}}{\text{Var}\{s\}} = \frac{\min_{\mathbf{p} \in \mathbb{C}^L} \mathbb{E} \{ |\mathbf{p}^H \mathbf{z} - s|^2 \}}{\text{Var}\{s\}}. \quad (15)$$

Finding the optimal eavesdropper strategy, thus, reduces to finding the optimal combining vector, which is presented in the following section.

III. SECURITY LEVEL ANALYSIS AND OPTIMAL EAVESDROPPER STRATEGY

In this section, we evaluate the security level under different side information assumptions and a special case with non-cooperating eavesdroppers (i.e., they are unaware of each other's existence). Additionally, we provide the optimal (eavesdropper) combining vectors when applicable.

A. Scenario 1: Exact CSI Known

Assuming that the channel coefficients between legitimate users and eavesdroppers are perfectly known to the eavesdroppers ($\Phi = \{\mathbf{g}_1, \dots, \mathbf{g}_L\}$), the security level in Definition 1 can be computed as follows.

Theorem 2. Consider the proposed OtA computation scheme with source data $\boldsymbol{\gamma} \sim \mathcal{CN}(\mathbf{0}, \mathbf{I}_K)$ and the cooperative eavesdropper strategy. The computation result is MSE-secure with security level

$$S = 1 - \frac{1}{K} \mathbf{m}^H \mathbf{B}^{-1} \mathbf{m},$$

and the optimal combining vector is

$$\mathbf{p}_{\text{opt}} = \mathbf{B}^{-1} \mathbf{m},$$

where

$$B = GAA^H G^H + \eta^2 G D_h^{-1} D_h^{-H} G^H + \sigma_z^2 I_L,$$

$$m = \eta G D_h^{-1} u = \begin{bmatrix} \eta \sum_{k=1}^K g_{1,k}/h_k \\ \eta \sum_{k=1}^K g_{2,k}/h_k \\ \vdots \\ \eta \sum_{k=1}^K g_{L,k}/h_k \end{bmatrix}, \quad u = \begin{bmatrix} 1 \\ \vdots \\ 1 \end{bmatrix}.$$

Proof. See Appendix B. \square

The matrix B consists of three terms, corresponding to the alignment between the artificial noise and the eavesdropper channels, the channel mismatch between legitimate users and eavesdroppers, and the additive noise, respectively. Intuitively, beamforming the artificial noise towards the eavesdropper channels improves the security.

Remark 3. After optimal combining, the virtual eavesdropper obtains the estimate

$$\hat{s} = p_{opt}^H z = p_{opt}^H G x + p_{opt}^H n_z = \tilde{g}^T x + \tilde{n}_z, \quad (16)$$

where $\tilde{g} = p_{opt}^H G$ can be viewed as the effective channel vector and $\tilde{n}_z \sim \mathcal{CN}(0, \sigma_z^2 \|p_{opt}\|^2)$ as additive noise. Then, using [48, Th.1], we can equivalently write the security level in Theorem 2 as

$$S = 1 - \frac{\frac{\eta^2}{K} \left| \sum_{k=1}^K \frac{\tilde{g}_k}{h_k} \right|^2}{\eta^2 \sum_{k=1}^K \left| \frac{\tilde{g}_k}{h_k} \right|^2 + \|\tilde{g}^T A\|^2 + \sigma_z^2 \|p_{opt}\|^2}. \quad (17)$$

B. Scenario 2: No Phase Information

It might be unrealistic to assume that the eavesdroppers have perfect knowledge of the channels between them and the legitimate users. Therefore, we now consider the scenario in which only statistical CSI is available. Consequently, the expectations in Definition 1 are taken over the randomness in G and h , in addition to other sources of randomness in the system. We consider random complex fading coefficients g_ℓ , with uniform phase distribution. In this case, we show that the security level is $S = 1$.

Theorem 3. If the channel coefficients $g_{\ell,k} = r_{\ell,k} \exp(-j\phi_{\ell,k})$ have a uniformly distributed phase, $\phi_{\ell,k} \sim \mathcal{U}([0, 2\pi])$, then the security level is $S = 1$.

Proof. Note that, for any ψ , the distributions of G and $e^{j\psi} G$ as well as γ and $e^{-j\psi} \gamma$ are the same. Let $p(\cdot)$ denote the probability density function of a continuous random variable. Then, for $\gamma' = e^{-j\psi} \gamma$, we have $p(\gamma) = p(\gamma')$ and $p(z|\gamma) = p(z|\gamma')$, and therefore $p(\gamma'|z) = p(z|\gamma')p(\gamma')/p(z) = p(z|\gamma)p(\gamma)/p(z) = p(\gamma|z)$. Consequently, the MMSE estimator of the data is $E[\gamma|z] = E[\gamma'|z] = e^{-j\psi} E[\gamma|z]$ for arbitrary ψ . The only possibility is $E[\gamma|z] = 0$, from which it follows that the MMSE estimator of s is $\mathbb{E}\{s|z\} = \mathbf{1}^T \mathbb{E}\{\gamma|z\} = 0$. The security level is thus $S = \frac{1}{\text{Var}\{s\}} \mathbb{E}\{|0 - s|^2\} = \text{Var}\{s\}/\text{Var}\{s\} = 1$. \square

Observing that 1 is the maximum achievable security level, we conclude that when only channel statistics are known to eavesdroppers, there is no need to add extra artificial noise to improve MSE-security in our considered setting. Therefore, in Section IV, we will focus on the case with known CSI when deriving the optimal artificial noise design.

C. Non-cooperative Eavesdroppers

In the event that the eavesdroppers are not cooperating, we define the security level as

$$S = \frac{1}{\text{Var}\{s\}} \min_{\ell \in (1, \dots, L)} \left(\min_{d_z: \mathbb{C} \rightarrow \mathbb{C}} \mathbb{E}\{|d_z(z_\ell; \Phi) - s|^2 | \Phi\} \right). \quad (18)$$

That is, the security at the eavesdropper with the lowest MSE. Using [48, Th.1], it can be computed as

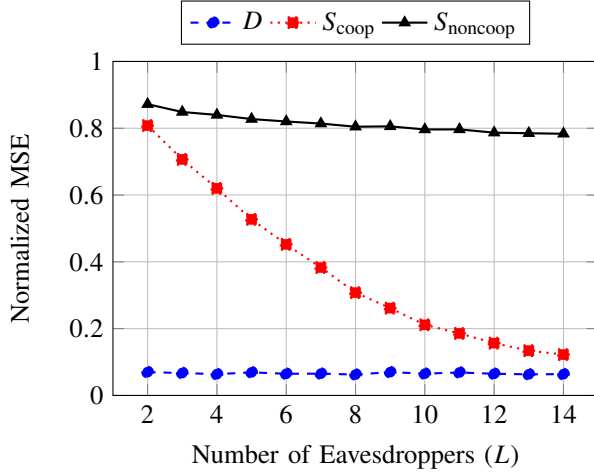
$$S = \min_{\ell \in (1, \dots, L)} \left(1 - \frac{\frac{\eta^2}{K} \left| \sum_{k=1}^K \frac{g_{k,\ell}}{h_k} \right|^2}{\eta^2 \sum_{k=1}^K \left| \frac{g_{k,\ell}}{h_k} \right|^2 + \|\mathbf{g}_\ell^T A\|^2 + \sigma_{z_\ell}^2} \right). \quad (19)$$

D. Inherent Security and Impact of Eavesdropper Cooperation

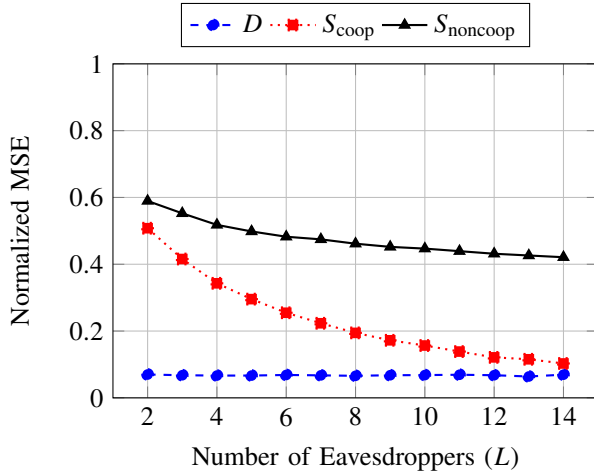
First, we simulate the system without artificial noise ($A = 0$) to evaluate its inherent security. The system consists of $K = 10$ users and a varying number of eavesdroppers. A detailed description of the simulation environment is provided in Section V. Fig. 3a shows the approximation error and security levels in the cooperative and non-cooperative cases, computed according to Theorem 2 and (19), respectively. It can be observed that the security level decreases significantly as the number of cooperating eavesdroppers L increases. Interestingly, the non-cooperative security level experiences only minimal degradation as L increases. Since the minimum security level across the eavesdroppers remains relatively constant with the increase in L , we conclude that all eavesdroppers must exhibit similarly poor aggregation accuracy.

In some earlier studies such as [48], the channel coefficients were modeled as real-valued random numbers. In this case, there is no phase misalignment in the received signals, and individual eavesdroppers can attain higher estimation accuracy. In practice, when I/Q modulation is used, the channel coefficients are modeled as complex-valued random numbers, where the phase of the signal carries information about the data symbols. Misaligned channel phases between the legitimate user channels and eavesdropper channels lead to a larger value in the numerator of (19). Consequently, the security level obtained with the complex-valued channel model is inherently higher than the real-valued case, as illustrated by the comparison between Fig. 3a and Fig. 3b.

Based on these results, we conclude that there is significant inherent security in OtA systems when eavesdroppers are not cooperating, induced by phase misalignment between the legitimate user and eavesdropper channels. Despite this, cooperation among distributed eavesdroppers evidently allows them to exploit their diversity effectively, posing a significant



(a) With complex-valued channels.



(b) With real-valued channels.

Fig. 3. Estimation accuracy of the server, cooperative eavesdroppers and non-cooperative eavesdroppers, in a scenario with no added artificial noise.

security threat as L increases.⁴ This motivates the introduction of carefully designed artificial noise, which aims at sustaining a performance gap between the server and eavesdroppers. The choice of η also affects this performance gap. However, in this work we consider that η has been chosen to satisfy some approximation error requirement, and focus on optimizing the artificial noise.

IV. ARTIFICIAL NOISE DESIGN

In this section, we address the question of how the artificial noise should be designed. The problem essentially reduces to designing the noise precoding matrix $\mathbf{A} \in \mathbb{C}^{K \times m}$ for some $m < K$. Despite the inherent security in the non-cooperative eavesdropper case, we provide an artificial noise design that optimizes the security in this scenario and subsequently shows that it achieves good security performance even in the cooperative case.

⁴Without channel noise, $L = K$ eavesdroppers can perfectly recover the source data values from K legitimate users, achieving error-free estimation.

The security level in the non-cooperative case given in (19) is maximized by solving

$$\max_{\mathbf{A}} \min_{\ell \in \{1, \dots, L\}} \frac{\eta^2 \sum_{k=1}^K \left| \frac{g_{k,\ell}}{h_k} \right|^2 + \|\mathbf{g}_\ell^T \mathbf{A}\|^2 + \sigma_{z_\ell}^2}{\left| \sum_{k=1}^K \frac{g_{k,\ell}}{h_k} \right|^2} \quad (20a)$$

$$\text{subject to } \|\mathbf{a}_k\|^2 \leq P - \eta^2/|h_k|^2, \forall k \in \{1, 2, \dots, K\}, \quad (20b)$$

$$\|\mathbf{h}^T \mathbf{A}\|^2 \leq \frac{\mu K \eta^2}{(1 - \mu)} - \sigma_y^2, \quad (20c)$$

where the constraints in (20b) and (20c) correspond to the power and approximation error constraints derived from the upper and lower bounds in Corollary 1, respectively. At each individual eavesdropper, the security is given as an affine function of the received noise power $\|\mathbf{g}_\ell^T \mathbf{A}\|^2$. The server maximizes the minimum security level across the eavesdroppers by beamforming the artificial noise in the direction of different eavesdroppers proportionally to their channel misalignments. In addition, there are two bias terms. The first term, $\eta^2 \sum_{k=1}^K \left| \frac{g_{k,\ell}}{h_k} \right|^2 / \left| \sum_{k=1}^K \frac{g_{k,\ell}}{h_k} \right|^2$, increases when the phase between \mathbf{g}_ℓ and \mathbf{h} are more misaligned. The second term, $\sigma_{z_\ell}^2 / \left| \sum_{k=1}^K \frac{g_{k,\ell}}{h_k} \right|^2$, decreases as the eavesdroppers' SNR increases. This interpretation suggests that we should focus the artificial noise towards eavesdroppers whose channel vectors are more aligned with \mathbf{h} and who have relatively good channel conditions.

The problem in (20) can be transformed to

$$\max_{t, \mathbf{A}} t \quad (21a)$$

subject to

$$\frac{\eta^2 \sum_{k=1}^K \left| \frac{g_{k,\ell}}{h_k} \right|^2 + \|\mathbf{g}_\ell^T \mathbf{A}\|^2 + \sigma_{z_\ell}^2}{\left| \sum_{k=1}^K \frac{g_{k,\ell}}{h_k} \right|^2} \geq t, \forall \ell \in \{1, \dots, L\} \quad (21b)$$

$$\|\mathbf{a}_k\|^2 \leq P - \eta^2/|h_k|^2, \forall k \in \{1, 2, \dots, K\}, \quad (21c)$$

$$\|\mathbf{h}^T \mathbf{A}\|^2 \leq \frac{\mu K \eta^2}{(1 - \mu)} - \sigma_y^2. \quad (21d)$$

Since the constraints are non-convex in \mathbf{A} , we propose a structured noise design that makes (21) efficiently solvable. Furthermore, the proposed design is zero-forcing, thereby inherently satisfying the approximation error constraint in (21d), assuming that the approximation error bound μ is achievable (in the noiseless case).⁵

⁵The optimization problem can be solved (in $\mathbf{Q} = \mathbf{A}\mathbf{A}^H$) using semidefinite relaxation. However, the low rank constraint on \mathbf{Q} , imposed by the tall shape of \mathbf{A} ($m < K$), complicates either the problem (if a rank constraint is imposed), or the extraction of \mathbf{A} from the potentially full rank \mathbf{Q} .

A. Proposed Noise Design

We consider zero-forcing noise designs. Although potentially sub-optimal, we motivate this choice by the observation that zero-forcing noise designs are among the top performers with regard to the security-approximation tradeoff (cf. Section V). In the spirit of [48], we choose $\mathbf{A} \in \mathbb{C}^{K \times (K-1)}$ in the form

$$\mathbf{A} = \begin{bmatrix} \mathbf{I}_{K-1} \\ -\frac{h_1}{h_K} \quad \dots \quad -\frac{h_{K-1}}{h_K} \end{bmatrix} \begin{bmatrix} \sqrt{\lambda_1} & & 0 \\ & \ddots & \\ 0 & & \sqrt{\lambda_{K-1}} \end{bmatrix} \\ = \begin{bmatrix} \mathbf{\Lambda}^{1/2} \\ -\sqrt{\lambda_1} \frac{h_1}{h_K} \quad \dots \quad -\sqrt{\lambda_{K-1}} \frac{h_{K-1}}{h_K} \end{bmatrix}, \quad (22)$$

where $\mathbf{\Lambda}^{1/2} = \text{diag}(\sqrt{\lambda_1}, \dots, \sqrt{\lambda_{K-1}})$. This noise design satisfies the zero-forcing condition, i.e., $\mathbf{h}^T \mathbf{A} = \mathbf{0}$, while allowing control over the power allocation through $(\lambda_1, \dots, \lambda_{K-1})$. Note that the responsibility to ensure zero-forcing falls on a single user. Without loss of generality, we assume that user K has the best channel condition and thus the most energy to allocate to the artificial noise. One key advantage of this design is that it performs particularly well when there is a large imbalance in the power allocated to artificial noise at different users. One such case is if η is chosen close to the upper bound. In this case, the user with the worst channel allocates little power to the artificial noise, forcing all elements of the corresponding row of \mathbf{A} to be small. However, to preserve its zero-forcing nature, the column span must not change in the process. With the proposed design, one row can be made arbitrarily small without limiting the noise generation at the other users. It may even enable them to transmit additional noise, as the K -th user has one less noise signal to compensate for. Conversely, a non-sparse (but still zero-forcing) design would necessitate scaling down the entire matrix and thus the artificial noise power of all users.

The design also offers advantages in terms of communication overhead. The general problem of broadcasting \mathbf{A} ($K^2 - K$ symbols) reduces to broadcasting $\mathbf{\Lambda}^{1/2}$ ($K - 1$ symbols) and sharing \mathbf{h} ($K - 1$ symbols, excluding h_K) with the K -th user.

With the proposed design, we have

$$\|\mathbf{g}_\ell^T \mathbf{A}\|^2 = \sum_{i=1}^{K-1} \lambda_i \left| g_{\ell,i} - g_{\ell,K} \frac{h_i}{h_K} \right|^2 \quad \forall \ell, \quad (23)$$

$$\|\mathbf{a}_k\|^2 = \begin{cases} \lambda_k, & \text{if } k \neq K \\ \sum_{i=1}^{K-1} \lambda_i \left| \frac{h_i}{h_K} \right|^2, & \text{otherwise} \end{cases}. \quad (24)$$

Then, it follows that

$$\frac{\eta^2 \sum_{k=1}^K \left| \frac{g_{k,\ell}}{h_k} \right|^2 + \|\mathbf{g}_\ell^T \mathbf{A}\|^2 + \sigma_z^2}{\left| \sum_{k=1}^K \frac{g_{k,\ell}}{h_k} \right|^2} = \alpha_\ell + \sum_{i=1}^{K-1} \beta_{\ell,i} \lambda_i, \quad (25)$$

where

$$\alpha_\ell = \frac{\eta^2 \sum_{k=1}^K \left| \frac{g_{k,\ell}}{h_k} \right|^2 + \sigma_z^2}{\left| \sum_{k=1}^K \frac{g_{k,\ell}}{h_k} \right|^2}, \quad \beta_{\ell,i} = \frac{\left| g_{\ell,i} - g_{\ell,K} \frac{h_i}{h_K} \right|^2}{\left| \sum_{k=1}^K \frac{g_{k,\ell}}{h_k} \right|^2}. \quad (26)$$

The original max-min problem can be transformed into the following optimization problem:

$$\max_{t, \lambda_1, \dots, \lambda_{K-1}} t \quad (27a)$$

$$\text{subject to} \quad \alpha_\ell + \sum_{i=1}^{K-1} \beta_{\ell,i} \lambda_i \geq t, \quad \forall \ell \in \{1, \dots, L\} \quad (27b)$$

$$\lambda_k \leq P - \eta^2 / |h_k|^2, \quad \forall k \in \{1, \dots, K-1\} \quad (27c)$$

$$\sum_{i=1}^{K-1} \lambda_i \left| \frac{h_i}{h_K} \right|^2 \leq P - \eta^2 / |h_K|^2 \quad (27d)$$

$$\lambda_i \geq 0, \quad \forall i \in \{1, \dots, K-1\}. \quad (27e)$$

The constraints in (27c) and (27d) correspond to the power constraints. Given that both the objective and the constraints are linear in $\lambda_1, \dots, \lambda_{K-1}$, the problem can be efficiently solved using linear programming techniques.

B. Distributing the Zero-forcing Responsibility

Additionally, we consider an extension where, rather than relying on a single user to ensure zero-forcing, this responsibility is shared among a subset of users \mathcal{Z} with cardinality $N = |\mathcal{Z}|$. Without loss of generality, we assume that the users are ordered such that the first $K - N$ users generate independent noise, and the last N users share the zero-forcing responsibility. Then, we construct $\mathbf{A} = \mathbf{A}' \mathbf{\Lambda}^{1/2} \in \mathbb{C}^{K \times (K-N)}$, where $\mathbf{\Lambda}^{1/2} = \text{diag}(\sqrt{\lambda_1}, \dots, \sqrt{\lambda_{K-N}})$ and

$$\mathbf{A}' = \begin{bmatrix} \mathbf{I}_{K-N} \\ -\frac{h_1}{h_{K-N+1}} d_{K-N+1} \quad \dots \quad -\frac{h_{K-N}}{h_{K-N+1}} d_{K-N+1} \\ \vdots \quad \vdots \quad \vdots \\ -\frac{h_1}{h_K} d_K \quad \dots \quad -\frac{h_{K-N}}{h_K} d_K \end{bmatrix}. \quad (28)$$

The weights d_{K-N+1}, \dots, d_K control each user's contribution to ensuring zero-forcing and must satisfy $\sum_{k=K-N+1}^K d_k = 1$. One option is to choose the weights proportional to the available power, i.e.,

$$d_k = \frac{P - \eta^2 / |h_k|^2}{NP - \eta^2 \sum_{j=K-N+1}^K |h_j|^{-2}}. \quad (29)$$

Following the same methodology as in the $N = 1$ case, we optimize \mathbf{A} by solving

$$\max_{\lambda_1, \dots, \lambda_{K-N}} t \quad (30a)$$

$$\text{subject to } \alpha_\ell + \sum_{i=1}^{K-N} \beta'_{\ell,i} \lambda_i \geq t, \forall \ell \in \{1, \dots, L\} \quad (30b)$$

$$\lambda_k \leq P - \eta^2 / |h_k|^2, \forall k \in \{1, \dots, K\} \setminus \mathcal{Z} \quad (30c)$$

$$\sum_{i=1}^{K-N} \lambda_i \left| d_k \frac{h_i}{h_k} \right|^2 \leq P - \eta^2 / |h_k|^2, \forall k \in \mathcal{Z} \quad (30d)$$

$$\lambda_i \geq 0, \forall i \in \{1, \dots, K-N\}, \quad (30e)$$

where

$$\beta'_{\ell,i} = \frac{\left| g_{\ell,i} - \sum_{j=K-N+1}^K g_{\ell,j} \frac{h_i}{h_j} d_j \right|^2}{\left| \sum_{k=1}^K \frac{g_{k,\ell}}{h_k} \right|^2}. \quad (31)$$

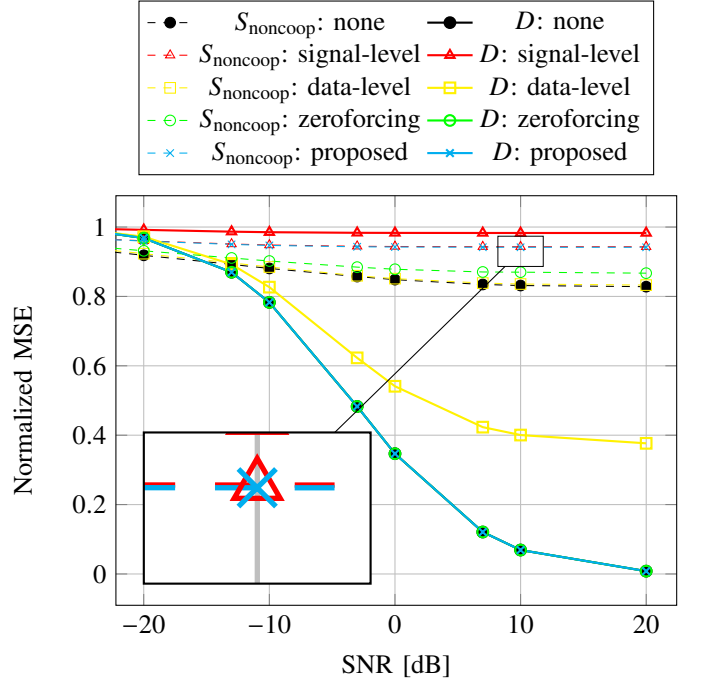
This design allows for a larger magnitude of artificial noise, at the cost of restricting the subspace in which the noise is generated, by reducing the rank of \mathbf{A} . In Section V, we illustrate the combined impact of these two aspects on the security level. Joint optimization of user selection (\mathcal{Z}), zero-forcing weights (d_{K-N+1}, \dots, d_K) and power allocation ($\mathbf{A}^{1/2}$) is left for future work.

V. SIMULATION RESULTS

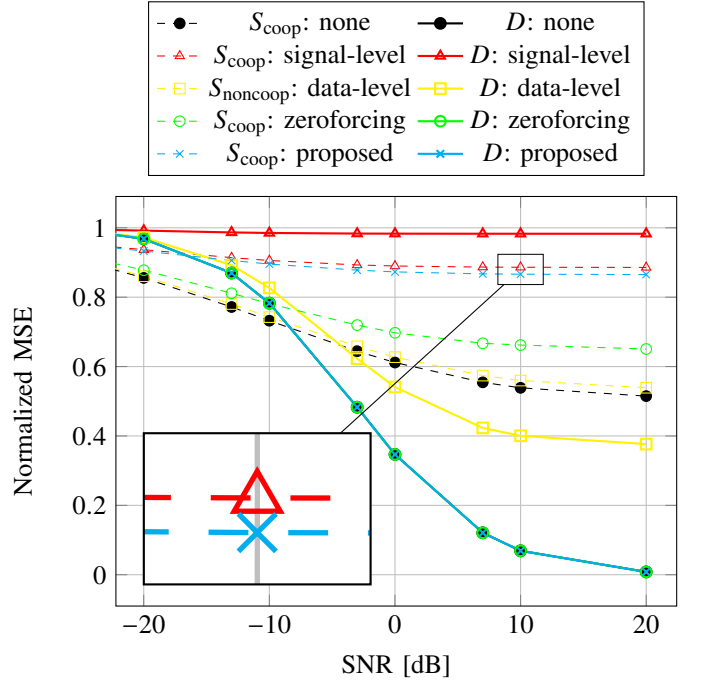
In this section, we evaluate the performance of the proposed artificial noise design for secure OtA computation, examine the effects of power control, and discuss the tradeoff between accuracy and security. The simulated system consists of $K = 10$ users and $L = 5$ eavesdroppers uniformly and randomly distributed in a disk of radius 100 m. The server is located in the center of the disk, and neither legitimate users nor eavesdroppers are located within 1 m of the server or of each other. All results are averaged over at least 100 realizations of random positions. Channel coefficients are modeled as random variables following $\mathcal{CN}(0, d^{-4})$, where d is the distance of the communication link. Stated SNR values are the average SNR with 100 m link distance. When unspecified, system parameters are configured to achieve an SNR of 10 dB. We consider the scenario where all small-scale fading coefficients are larger than 0.1, which can be achieved by only scheduling users with sufficiently good channel conditions to participate in the aggregation.

A. Effects of Artificial Noise Design

Existing approaches in the literature largely rely on transmitting uncorrelated Gaussian artificial noise, and can be broadly classified into two categories: 1) adding noise before signal scaling (e.g., DP-achieving schemes) [34], [35], [49], and 2) adding noise after scaling, leveraging the residual power not reserved for data transmission (e.g., schemes with friendly jammers) [41], [42], [48]. These are referred to as data- and signal-level noise, respectively, in the following



(a) With non-cooperative eavesdroppers.



(b) With cooperative eavesdroppers.

Fig. 4. Performance comparison between the server and eavesdroppers, for different noise designs.

results.⁶ Fig. 4a illustrates how the addition of artificial noise impacts the approximation error and security level in the non-cooperative case. Five different noise designs are implemented and compared:

- none : $\mathbf{A} = 0$.

⁶Direct comparison with existing secure OtA FL schemes is challenging due to different design objectives and performance metrics, cf. Section I-A.

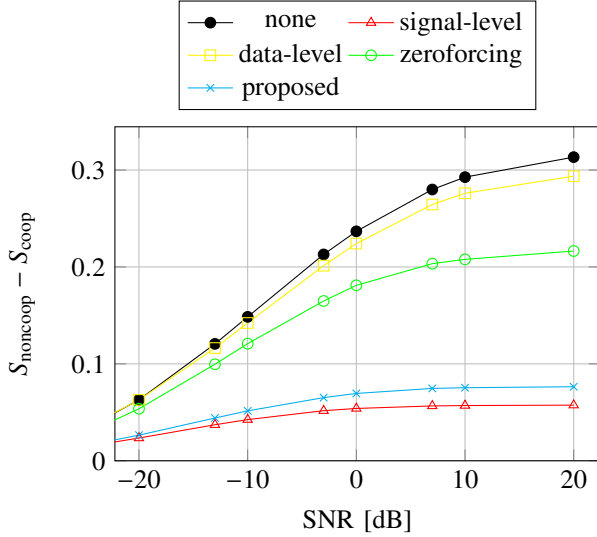


Fig. 5. Security gap between cooperative and non-cooperative eavesdroppers. Each curve is the difference between the non-cooperative and cooperative security level for that given noise scheme.

- `signal-level` : Each user independently transmits Gaussian noise with variance $P - \eta^2/|h_k|^2$.
- `data-level` : Each user independently adds Gaussian noise prior to scaling the signal.
- `zeroforcing` : Random zero-forcing design. \mathbf{A} is chosen as a random $K \times (K - 1)$ matrix that spans the entire nullspace of \mathbf{h} , multiplied by a scalar so that all rows satisfy their respective power constraints.
- `proposed` : the optimized zero-forcing design computed according to (27).

All noise designs are simulated using the same η value. The uncorrelated signal-level noise design achieves the highest security level since it leverages all available residual power as opposed to the other schemes. Conversely, not adding any artificial noise can achieve the lowest approximation error.

By design, zero-forcing approaches (including the proposed design) achieve the same approximation error as in the case without artificial noise. From a security perspective, the proposed method performs almost as well as the signal-level uncorrelated noise design, even though zero-forcing methods (and the data-level uncorrelated design) requires some users not to transmit with full power, to preserve the column span of \mathbf{A} and fair aggregation, respectively.

In Fig. 4b, we validate the performance of the proposed artificial noise design in the scenario with cooperating eavesdroppers. Similar to the non-cooperative case, the proposed design achieves security that approaches the case with signal-level uncorrelated noise. Additionally, it is worth noting that the proposed noise design closes the gap between the security levels in the non-cooperative and cooperative cases, respectively, which is further illustrated in Fig. 5. The advantage gained by the eavesdroppers through cooperation is significantly diminished under the proposed noise scheme.

From the plots corresponding to uncorrelated noise in Figs. 4a and 4b, it is evident that random perturbations disproportionately harm the aggregation accuracy at the server. This

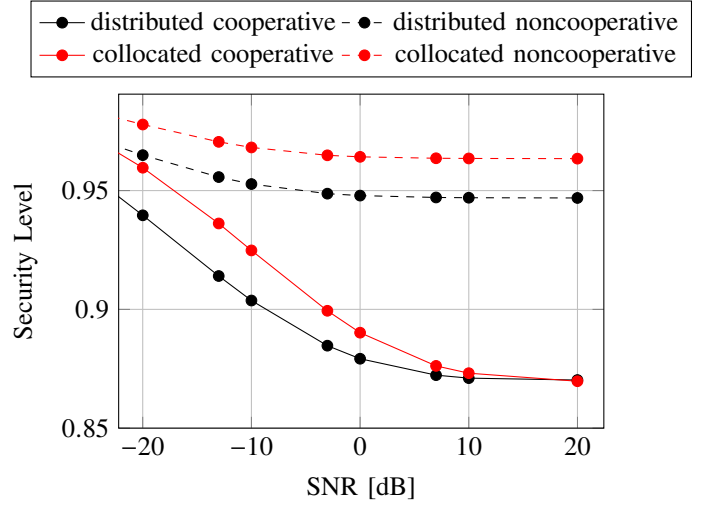


Fig. 6. Cooperative and non-cooperative security levels with collocated and distributed eavesdroppers.

is reasonable since cooperative eavesdroppers have multiple observations of the same perturbation signal, which can be exploited to obtain a more accurate estimate of the target function value. This is the motivating observation behind the decision to optimize the noise precoding matrix across zero-forcing designs specifically.

B. Effects of Spatially Distributed Eavesdroppers

Some prior studies consider a single multiple-antenna eavesdropper [43]–[45]. Figure 6 illustrates the security levels for the cooperative and non-cooperative cases with L distributed single-antenna eavesdroppers compared to a single eavesdropper with L antennas (collocating the eavesdroppers). We observe that the distributed eavesdropper scenario considered in this paper constitutes a more challenging scenario in terms of ensuring a certain security level.

C. Effects of Different Numbers of Zero-Forcing Users

Fig. 7 compares the average security levels with artificial noise computed according to (27) and (30), respectively. The $N=1$ and $N=2$ curves are generated with optimal user selection found by exhaustive search. That is, for each channel realization, we solve (30) for all possible subsets of N users \mathcal{Z} , and choose the solution that gives the largest security level. Whereas, `proposed` uses $\mathcal{Z} = \{\arg \max_k |h_k|^2\}$. The small gap between the proposed and $N=1$ designs indicates that, if selecting a single user to ensure the zero-forcing condition, selecting the user with best channel condition is close to optimal in most cases. The almost negligible security increase does not warrant the increased computational cost of constructing and evaluating multiple noise precoding matrices. When selecting multiple zero-forcing users, the gain depends on the number of eavesdroppers. For smaller values of L , where the eavesdropper channels span a smaller subspace, reducing the artificial noise's dimensionality (e.g., $K - N = 8$ dimensions for $N=2$) has a relatively small impact. In turn,

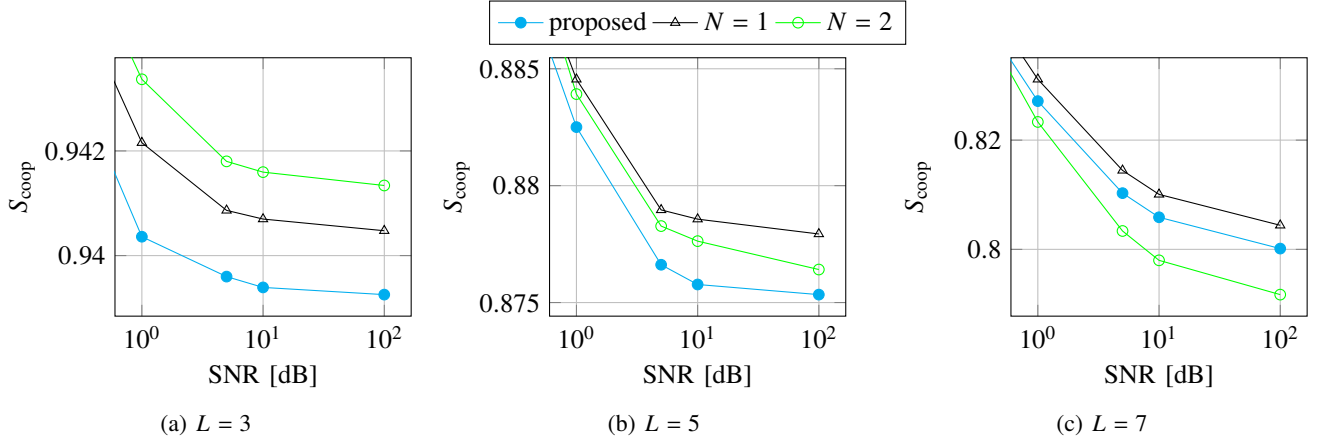


Fig. 7. Security level with different numbers of users ensuring zero-forcing in the proposed design, for different values of L .

it allows for an increased artificial noise amplitude, thus, improving the security level overall. Conversely, for $L = 7$, the increased magnitude of artificial noise generally fails to compensate for the reduction in security due to limiting the rank of \mathbf{A} . Nevertheless, it can be observed that $N = 2$ outperforms $N = 1$ for some channel realizations, suggesting that, even in this scenario, a scheme that adaptively chooses an optimal subset \mathcal{Z} (including the value of N) can achieve even better performance. However, this requires an additional design to efficiently find the optimal user selection. In the remaining results, we only consider the case with one zero-forcing user, i.e., the design given in (27).

D. Effects of Power Control

Fig. 8 shows the impact of power control on the security level and approximation error, with the proposed noise design. We represent the amplitude scaling factor equivalently by the fraction $\delta \in [0, 1]$ of the maximum value, that is, $\eta = \delta \min_{k \in \{1, 2, \dots, K\}} P |h_k|^2$ (cf. Corollary 1). With sufficient available power, it is possible to greatly improve security (by decreasing η) without significantly impacting the approximation error.

E. Achievable Security-Accuracy Tradeoffs

To better understand the security-accuracy trade-off, Fig. 9 numerically approximates the achievable pairs of security level and approximation error by Monte Carlo simulation. L and the SNR are set to 7 and 0 dB, respectively. Only configurations above the diagonal are of potential interest, as they represent cases where the server achieves better estimation accuracy than the eavesdroppers. Noting that every artificial noise design can be decomposed into a zero-forcing part and a non-zero-forcing part, we generate random pairs of zero-forcing and non-zero-forcing noise designs and obtain mixtures by interpolating between them. This is repeated for 40 equidistant values of δ in the range $[0, 1]$.

It is possible that a random zero-forcing matrix achieves better security than the proposed scheme due to the large number of generated matrices. However, it is clear that the proposed design is among the top performers. Additionally, the

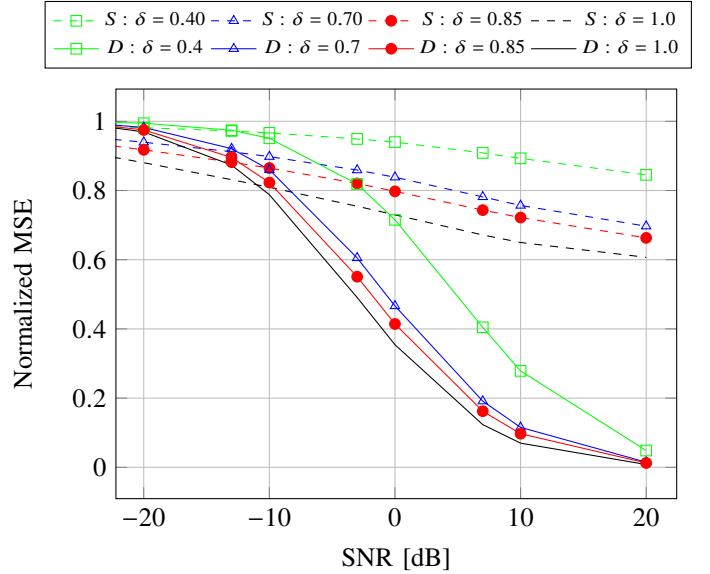


Fig. 8. Security level and approximation error with the proposed noise design for different amplitude scaling factors.

proposed design can be found efficiently by solving a linear programming problem, which is preferred over generating and evaluating a large number of random designs in practice. The proposed design performs particularly well when considering low approximation errors, or equivalently, high accuracy requirements at the server. In this regime, η is large, leaving relatively little energy for artificial noise, necessitating careful use of the available power.

VI. CONCLUSIONS

In this work, we investigated secure OtA computation in the presence of multiple (potentially cooperating) eavesdroppers by injecting correlated artificial noise at multiple source nodes to obscure their transmitted data signals. We provided fundamental bounds on the estimation performance of the server/receiver and the eavesdroppers, and derived the optimal joint estimator for cooperative eavesdroppers. Furthermore, we proposed an optimized zero-forcing noise design, which

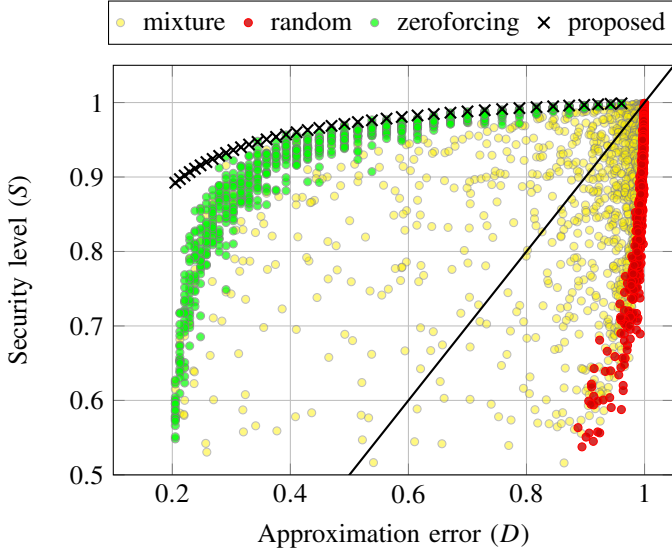


Fig. 9. Achievable pairs of security level and approximation error for a given realization of the system.

was shown to achieve good performance under the accuracy-security tradeoff. Our main takeaway messages are as follows: 1) In analog function computation over wireless channels, random phase rotation during signal transmission can provide inherent MSE-security against potential eavesdropping; 2) This inherent security diminishes when multiple eavesdroppers are able to cooperate to improve their estimate of the intended computation result; 3) Introducing correlated artificial noise with an optimized structure can substantially enhance security against eavesdropping without compromising the aggregation accuracy at the server.

ACKNOWLEDGMENTS

This work was supported in part by Zenith, ELLIIT, Swedish Research Council (VR), Knut och Alice Wallenbergs stiftelse (KAW), and Wallenberg AI, Autonomous Systems and Software Program (WASP) funded by the Knut and Alice Wallenberg Foundation, and by the Bavarian Ministry of Economic Affairs, Regional Development and Energy within the scope of the 6G Future Lab Bavaria.

APPENDIX A PROOF OF THEOREM 1

The approximation error is

$$D = \min_{d_y: \mathbb{C} \rightarrow \mathbb{C}} \frac{\mathbb{E} \{|d_y(y; \Phi) - s|^2\}}{\text{Var}\{s\}},$$

where $s = \sum_{k=1}^K \gamma_k$ and $y = \eta s + \mathbf{h}^T \mathbf{A} \mathbf{v} + n_y$. Since, s and y are jointly Gaussian,

$$\mathbb{E} \{|d_y(y; \Phi) - s|^2\} = \text{Var}\{s\} - \text{Cov}[s, y] \text{Var}\{y\}^{-1} \text{Cov}[y, s],$$

and consequently

$$D = 1 - \frac{\text{Cov}[s, y] \text{Cov}[y, s]}{\text{Var}\{y\} \text{Var}\{s\}}.$$

Since n_y and all elements in γ and \mathbf{v} are independent random variables with zero mean and unit variance, we have

$$\begin{aligned} \text{Var}\{s\} &= K, \\ \text{Var}\{y\} &= \text{Var}\{\eta s\} + \text{Var}\{\mathbf{h}^T \mathbf{A} \mathbf{v}\} + \text{Var}\{n_y\} \\ &= \eta^2 K + \|\mathbf{h}^T \mathbf{A}\|^2 + \sigma_y^2, \\ \text{Cov}[s, y] &= \text{Cov}[y, s]^* = \mathbb{E} \left\{ \left(\eta s + \mathbf{h}^T \mathbf{A} \mathbf{v} + n_y \right) s^* \right\} \\ &= \mathbb{E} \{ \eta s s^* \} = \eta K, \end{aligned}$$

from which the theorem follows. \square

APPENDIX B PROOF OF THEOREM 2

The MMSE estimator of s is given by:

$$\hat{s} = \mathbb{E} \{s | \mathbf{z}\},$$

where $\mathbf{z} = (z_1, \dots, z_L)^T$ contains the received signals at the eavesdroppers. Furthermore, since s and \mathbf{z} are jointly Gaussian, the MMSE estimator is linear and can be computed as

$$\hat{s} = \mathbb{E} \{s\} + \text{Cov}[s, \mathbf{z}] \text{Cov}[\mathbf{z}, \mathbf{z}]^{-1} \mathbf{z} = \mathbb{E} \{s \mathbf{z}^H\} \mathbb{E} \{\mathbf{z} \mathbf{z}^H\}^{-1} \mathbf{z}.$$

The corresponding MSE is

$$\begin{aligned} \text{Var}\{s | \mathbf{z}\} &= \text{Var}\{s\} - \text{Cov}[s, \mathbf{z}] \text{Cov}[\mathbf{z}, \mathbf{z}]^{-1} \text{Cov}[\mathbf{z}, s] \\ &= \text{Var}\{s\} - \mathbb{E} \{s \mathbf{z}^H\} \mathbb{E} \{\mathbf{z} \mathbf{z}^H\}^{-1} \mathbb{E} \{\mathbf{z} s^*\}, \end{aligned}$$

since both s and \mathbf{z} have zero mean. Given the expressions of s and \mathbf{z} written as

$$\begin{aligned} s &= \mathbf{u}^T \gamma, \\ \mathbf{z} &= \eta \mathbf{G} \mathbf{D}_{\mathbf{h}}^{-1} \gamma + \mathbf{G} \mathbf{A} \mathbf{v} + \mathbf{n}_z, \end{aligned}$$

since all elements in γ , \mathbf{v} and \mathbf{n}_z are independent random variables with zero mean and unit variance, we have

$$\begin{aligned} \text{Var}\{s\} &= K, \\ \mathbb{E} \{s \mathbf{z}^H\} &= \eta \mathbf{u}^T \mathbf{D}_{\mathbf{h}}^{-H} \mathbf{G}^H, \\ \mathbb{E} \{\mathbf{z} s^*\} &= \eta \mathbf{G} \mathbf{D}_{\mathbf{h}}^{-1} \mathbf{u}, \\ \mathbb{E} \{\mathbf{z} \mathbf{z}^H\} &= \eta^2 \mathbf{G} \mathbf{D}_{\mathbf{h}}^{-1} \mathbf{D}_{\mathbf{h}}^{-H} \mathbf{G}^H + \mathbf{G} \mathbf{A} \mathbf{A}^H \mathbf{G}^H + \sigma_z^2 \mathbf{I}_L. \end{aligned}$$

From this, the security level can be derived, and we get

$$\mathbf{p}_{\text{opt}} = \left(\mathbb{E} \{s \mathbf{z}^H\} \mathbb{E} \{\mathbf{z} \mathbf{z}^H\}^{-1} \right)^H = \mathbb{E} \{\mathbf{z} \mathbf{z}^H\}^{-1} \mathbb{E} \{\mathbf{z} s^*\}.$$

\square

REFERENCES

- [1] B. McMahan, E. Moore, D. Ramage, S. Hampson, and A. y. A. Blaise, "Communication-efficient learning of deep networks from decentralized data," in *Proceedings of the 20th International Conference on Artificial Intelligence and Statistics*. PMLR, Apr. 2017, pp. 1273–1282.
- [2] B. Nazer and M. Gastpar, "Computation over multiple-access channels," *IEEE Transactions on Information Theory*, vol. 53, no. 10, pp. 3498–3516, 2007.
- [3] M. Goldenbaum, H. Boche, and S. Stańczak, "Harnessing interference for analog function computation in wireless sensor networks," *IEEE Transactions on Signal Processing*, vol. 61, no. 20, pp. 4893–4906, 2013.
- [4] G. Zhu, J. Xu, K. Huang, and S. Cui, "Over-the-air computing for wireless data aggregation in massive IoT," *IEEE Wireless Communications*, vol. 28, no. 4, pp. 57–65, 2021.

- [5] Z. Chen, E. G. Larsson, C. Fischione, M. Johansson, and Y. Malitsky, "Over-the-air computation for distributed systems: Something old and something new," *IEEE Network*, vol. 37, no. 5, pp. 240–246, 2023.
- [6] Z. Wang, Y. Zhao, Y. Zhou, Y. Shi, C. Jiang, and K. B. Letaief, "Over-the-air computation for 6G: Foundations, technologies, and applications," *IEEE Internet of Things Journal*, vol. 11, no. 14, pp. 24634–24658, 2024.
- [7] L. Chen, N. Zhao, Y. Chen, F. R. Yu, and G. Wei, "Over-the-air computation for IoT networks: Computing multiple functions with antenna arrays," *IEEE Internet of Things journal*, vol. 5, no. 6, pp. 5296–5306, 2018.
- [8] X. Cao, G. Zhu, J. Xu, and K. Huang, "Optimized power control for over-the-air computation in fading channels," *IEEE Transactions on Wireless Communications*, vol. 19, no. 11, pp. 7498–7513, 2020.
- [9] K. Yang, T. Jiang, Y. Shi, and Z. Ding, "Federated learning via over-the-air computation," *IEEE Transactions on Wireless Communications*, vol. 19, no. 3, pp. 2022–2035, 2020.
- [10] X. Cao, G. Zhu, J. Xu, Z. Wang, and S. Cui, "Optimized power control design for over-the-air federated edge learning," *IEEE Journal on Selected Areas in Communications*, vol. 40, no. 1, pp. 342–358, 2021.
- [11] G. Zhu, Y. Wang, and K. Huang, "Broadband analog aggregation for low-latency federated edge learning," *IEEE Transactions on Wireless Communications*, vol. 19, no. 1, pp. 491–506, Jan. 2020.
- [12] M. M. Amiri and D. Gündüz, "Federated learning over wireless fading channels," *IEEE Transactions on Wireless Communications*, vol. 19, no. 5, pp. 3546–3557, May 2020.
- [13] M. F. U. Abrar and N. Michelusi, "Biased over-the-air federated learning under wireless heterogeneity," in *IEEE International Conference on Communications Workshops (ICC Workshops)*, 2024, pp. 111–116.
- [14] A. Şahin and R. Yang, "A survey on over-the-air computation," *IEEE Communications Surveys & Tutorials*, vol. 25, no. 3, pp. 1877–1908, 2023.
- [15] J. Katz and Y. Lindell, *Introduction to modern cryptography: principles and protocols*. Chapman and Hall/CRC, 2007.
- [16] M. Bloch and J. Barros, *Physical-layer security: from information theory to security engineering*. Cambridge University Press, 2011.
- [17] A. Mukherjee, "Physical-layer security in the internet of things: Sensing and communication confidentiality under resource constraints," *Proceedings of the IEEE*, vol. 103, no. 10, pp. 1747–1761, 2015.
- [18] A. D. Wyner, "The wire-tap channel," *Bell System Technical Journal*, vol. 54, no. 8, pp. 1355–1387, 1975.
- [19] E. Ekrem and S. Ulukus, "Capacity-equivocation region of the gaussian MIMO wiretap channel," *IEEE Transactions on Information Theory*, vol. 58, no. 9, pp. 5699–5710, Sep. 2012.
- [20] M. H. Yassaee and M. R. Aref, "Multiple access wiretap channels with strong secrecy," in *IEEE Information Theory Workshop*, 2010, pp. 1–5.
- [21] X. Guo, A. S. Leong, and S. Dey, "Estimation in wireless sensor networks with security constraints," *IEEE Transactions on Aerospace and Electronic Systems*, vol. 53, no. 2, pp. 544–561, 2017.
- [22] C. Goken, S. Gezici, and O. Arikan, "Estimation theoretic optimal encoding design for secure transmission of multiple parameters," *IEEE Transactions on Signal Processing*, vol. 67, no. 16, pp. 4302–4316, 2019.
- [23] D. Guo, S. Shamai, and S. Verdú, "Mutual information and minimum mean-square error in gaussian channels," *IEEE Transactions on Information Theory*, vol. 51, no. 4, pp. 1261–1282, 2005.
- [24] T. M. Cover and J. A. Thomas, *Elements of Information Theory*. John Wiley & Sons, Ltd, 2005. [Online]. Available: <https://onlinelibrary.wiley.com/doi/abs/10.1002/047174882X>
- [25] H. Reboredo, J. Xavier, and M. R. D. Rodrigues, "Filter design with secrecy constraints: The MIMO gaussian wiretap channel," *IEEE Transactions on Signal Processing*, vol. 61, no. 15, pp. 3799–3814, Aug. 2013.
- [26] J. Yang, I.-M. Kim, and D. I. Kim, "Optimal cooperative jamming for multiuser broadcast channel with multiple eavesdroppers," *IEEE Transactions on Wireless Communications*, vol. 12, no. 6, pp. 2840–2852, 2013.
- [27] A. Özçelikkale and T. M. Duman, "Cooperative precoding and artificial noise design for security over interference channels," *IEEE Signal Processing Letters*, vol. 22, no. 12, pp. 2234–2238, 2015.
- [28] M. Pei, J. Wei, K.-K. Wong, and X. Wang, "Masked beamforming for multiuser MIMO wiretap channels with imperfect CSI," *IEEE Transactions on Wireless Communications*, vol. 11, no. 2, pp. 544–549, 2012.
- [29] S. Goel and R. Negi, "Guaranteeing secrecy using artificial noise," *IEEE Transactions on Wireless Communications*, vol. 7, no. 6, pp. 2180–2189, Jun. 2008.
- [30] A. L. Swindlehurst, "Fixed SINR solutions for the MIMO wiretap channel," in *IEEE International Conference on Acoustics, Speech and Signal Processing*, 2009, pp. 2437–2440.
- [31] A. Khisti, G. Wornell, A. Wiesel, and Y. Eldar, "On the gaussian MIMO wiretap channel," in *IEEE International Symposium on Information Theory*, Jun. 2007, pp. 2471–2475.
- [32] S. Asoodeh, F. Alajaji, and T. Linder, "Privacy-aware MMSE estimation," in *IEEE International Symposium on Information Theory (ISIT)*, 2016, pp. 1989–1993.
- [33] C. Dwork, A. Roth et al., "The algorithmic foundations of differential privacy," *Foundations and trends® in theoretical computer science*, vol. 9, no. 3–4, pp. 211–407, 2014.
- [34] M. Seif, R. Tandon, and M. Li, "Wireless federated learning with local differential privacy," in *IEEE International Symposium on Information Theory (ISIT)*, 2020, pp. 2604–2609.
- [35] D. Liu and O. Simeone, "Privacy for free: Wireless federated learning via uncoded transmission with adaptive power control," *IEEE Journal on Selected Areas in Communications*, vol. 39, no. 1, pp. 170–185, 2021.
- [36] B. Hasircioğlu and D. Gündüz, "Communication efficient private federated learning using dithering," in *IEEE International Conference on Acoustics, Speech and Signal Processing (ICASSP)*, 2024, pp. 7575–7579.
- [37] Y. Tao, S. Chen, C. Zhang, D. Wang, D. Yu, X. Cheng, and F. Dressler, "Private over-the-air federated learning at band-limited edge," *IEEE Transactions on Mobile Computing*, vol. 23, no. 12, pp. 12444–12460, 2024.
- [38] S. Park and W. Choi, "On the differential privacy in federated learning based on over-the-air computation," *IEEE Transactions on Wireless Communications*, vol. 23, no. 5, pp. 4269–4283, 2023.
- [39] H. Liu, J. Yan, and Y.-J. A. Zhang, "Differentially private over-the-air federated learning over mimo fading channels," *IEEE Transactions on Wireless Communications*, vol. 23, no. 8, pp. 8232–8247, 2024.
- [40] B. Xiao, X. Yu, W. Ni, X. Wang, and H. V. Poor, "Over-the-air federated learning: Status quo, open challenges, and future directions," *Fundamental Research*, 2024.
- [41] B. He, F. Wang, Z. Chen, G. Zhang, and T. Q. S. Quek, "Secure over-the-air computation for wireless sensor network," *IEEE Communications Letters*, vol. 28, no. 11, pp. 2503–2507, 2024.
- [42] M. Frey, I. Bjelaković, and S. Stańczak, "Towards secure over-the-air computation," in *IEEE International Symposium on Information Theory (ISIT)*, 2021, pp. 700–705.
- [43] C. Hu, Q. Li, Q. Zhang, and J. Qin, "Secure transceiver design and power control for over-the-air computation networks," *IEEE Communications Letters*, vol. 26, no. 7, pp. 1509–1513, 2022.
- [44] H. Luo, Q. Li, Q. Zhang, and J. Qin, "Joint secure transceiver design for an untrusted MIMO relay assisted over-the-air computation networks with perfect and imperfect CSI," *IEEE Transactions on Information Forensics and Security*, vol. 18, pp. 2508–2523, 2023.
- [45] J. Yao, T. Wu, Q. Li, C. Pan, M. Jin, M. Elkhassan, X. Wang, and C. Yuen, "Secure beamforming optimization for IRS-assisted MIMO over-the-air computation networks," *IEEE Transactions on Communications*, pp. 1–1, 2025.
- [46] N. Yan, K. Wang, K. Zhi, C. Pan, K. K. Chai, and H. V. Poor, "Secure and private over-the-air federated learning: Biased and unbiased aggregation design," *IEEE Transactions on Wireless Communications*, vol. 24, no. 7, pp. 5901–5916, 2025.
- [47] M. Goldenbaum, H. Boche, and H. V. Poor, "Secure computation of linear functions over linear discrete multiple-access wiretap channels," in *50th Asilomar Conference on Signals, Systems and Computers*, pp. 1670–1674.
- [48] L. Maňny and A. Wachter-Zeh, "Secure over-the-air computation using zero-forced artificial noise," in *IEEE Information Theory Workshop (ITW)*, 2023, pp. 221–226.
- [49] J. Liao, Z. Chen, and E. G. Larsson, "Over-the-air federated learning with privacy protection via correlated additive perturbations," in *58th Annual Allerton Conference on Communication, Control, and Computing (Allerton)*, pp. 1–8.
- [50] U. Iqbal, S. Cho, H. Jung, and M. Guizani, "Performance analysis of physical layer security for over-the-air computation using distributed null-steering beamforming," *IEEE Communications Letters*, vol. 29, no. 2, pp. 303–307, 2025.
- [51] B. Hajek, *Random processes for engineers*. Cambridge University Press, 2015.